TOYOHASHI UNIVERSITY OF TECHNOLOGY

UNSTEADY TWO-DIMENSIONAL ORIFICE FLOW: AN EXPERIMENTAL INVESTIGATION

by

HUBERT CHANSON

SHIN-ICHI AOKI

MAMORU MARUYAMA

COASTAL/OCEAN ENGINEERING REPORT
NO. COE00-1

DEPARTMENT OF ARCHITECTURE AND CIVIL ENGINEERING

January 2000

UNSTEADY TWO-DIMENSIONAL ORIFICE FLOW: AN EXPERIMENTAL INVESTIGATION

by

Hubert CHANSON

Department of Civil Engineering, The University of Queensland, Brisbane QLD 4072, Australia (e-mail: h.chanson@mailbox.uq.edu.au)

Shin-ichi AOKI

Department of Architecture and Civil Engineering, Toyohashi University of Technology, Toyohashi 441-8580, Japan (e-mail: aoki@jughead.tutrp.tut.ac.jp)

Mamoru MARUYAMA

Department of Architecture and Civil Engineering, Toyohashi University of Technology, Toyohashi 441-8580, Japan

January, 2000

Abstract :

Orifice flows were used as water clocks since the Antiquity up to the 16-th century. Today the sand glass uses the same principle with granular material. Orifices and nozzles are used also as measuring discharges. A related form is the sharp-crested weir commonly used for discharge measurement in open channels. Most works were conducted with steady flow conditions and there is little information on the unsteady flow pattern. In this study, the writers describe an experimental investigation of an unsteady orifice flow. The study was conducted in a large-size facility with a rectangular orifice (0.75-m by 0.07-m) discharging up to 1.2 m^3 in about 10 seconds. The study is focused on the unsteady flow patterns, the discharge capacity and the velocity field in the reservoir. The results are compared with "classical" orifice flow results.

Abstract (in Japanese) :

今日でも使われている砂時計と同じ原理を用いて，オリフィス流れは古代から１６世紀頃まで水時計として使われていた．また，開水路流れの流量測定に刃形ぜきが用いられるように，オリフィスやノズルは流量の測定にも用いられてきた．

オリフィス流れに関するこれまでの研究のほとんどは定常流れを対象にしたもので，非定常流れに関する研究はほとんど見られない．本研究では，0.75m×0.07mの長方形オリフィスから10秒間に1.2m^{3}まで流出させることのできる大型の実験装置を用いて，オリフィスからの流出実験を行った．実験は，流れのパターンの非定常性，流出特性，および貯水タンク内の流れ場の特性に着目して行った．実験結果は古典的なオリフィス流れの理論や実験結果と比較した．

NOTATION

The following symbols are used in this report :

A	jet cross-section area (m^2);
A_o	orifice cross-section area (m2);
B	free-falling nappe width (m);
b	free-falling nappe thickness (m);
B_o	orifice width (m) (long dimension);
b_o	orifice thickness (m) (small dimension);
C_D	orifice discharge coefficient: $C_D = C_c * C_v$;
C_D'	corrected discharge coefficient;
C_c	orifice flow contraction coefficient: $C_c = A/A_o$;
C_v	orifice flow velocity coefficient;
g	gravity constant (m/s^2);
H	total head above orifice (m);
H_1	initial total head above orifice (m);
Q	total volume discharge (m^3/s) of water;
q	discharge per meter width (m^2/s) : at the orifice $q = Q/B_o$;
t	time (s);
t_1, t_2	times (s);
V	velocity (m/s);
V_x, V_y, V_z	velocity components (m/s) in the x-, y- and z-directions
x	horizontal Cartesian co-ordinate (m) along the short orifice dimension; $x = 0$ at orifice centreline;
y	horizontal Cartesian co-ordinate (m) along the orifice width; $y = 0$ at orifice centreline;
z	vertical Cartesian co-ordinate (m) positive upwards; $z = 0$ at the orifice;

Greek symbols

δ	convergence angle into the orifice;
μ	water dynamic viscosity (Pa.s);
ν	water kinematic viscosity (m^2/s) : $\nu = \mu/\rho$;
π	$\pi = 3.14159265358979323846264 3$;
θ_x	lateral spread angle of the bursting flow in the x-direction;
θ_y	lateral spread angle of the bursting flow in the y-direction;
ρ	water density (kg/m^3);
$\varnothing$	diameter (m);

Subscript

o	orifice reference conditions;
x	horizontal co-ordinate;
y	horizontal co-ordinate;

z	vertical co-ordinate;
1	initial flow conditions.

1. INTRODUCTION

Orifice flows were used as water clock ([1]) in ancient Babylon and Egypt ([2]) as well as in parts of Africa and by some North America Indians (Fig. 1-1). They were in use up to the 16-th century. Today the sand glass ([3]) uses the same principle with granular material. Orifices and nozzles are used also as measuring discharges. In his study of orifice flows, J.C. de BORDA (1733-1799) ([4]) made a significant contribution by not only introducing the concept of streamlines but also by developing the "Borda" mouthpiece to measure accurately the orifice flow. A related form of orifice is the sharp-crested weir commonly used for discharge measurement in open channels. When water flow through a sharp-edged orifice, the jet flow contracts to have its smallest section a small distance downstream of the hole. For a horizontal jet, Bernoulli principle implies that the velocity at vena contracta equals $\sqrt{2*g*H}$ where H is the reservoir head above orifice centreline ([5]). By continuity, the orifice discharge equals:

$$Q = C_D * A_0 * \sqrt{2 * g * H} \qquad (1\text{-}1)$$

where A_0 is the orifice cross-section area. The discharge coefficient C_D may be expressed as:

$$C_D = C_c * C_v \qquad (1\text{-}2)$$

where the velocity coefficient C_v account for the energy losses and the contraction coefficient C_c equals A/A_0, A being the jet cross-section area at vena contracta. For a horizontal water jet discharging from an infinite reservoir, C_c equals 0.58 and 0.61 for axisymmetrical and two-dimensional jets respectively ([6]). The value of C_c increases with increasing relative nozzle area when the reservoir is of finite dimensions.

Most works were conducted with steady flow conditions and there is little information on the unsteady flow pattern. In this report, the writers describe an experimental investigation of an unsteady orifice flow. The study was conducted in a large-size facility with a rectangular orifice (0.75-m by 0.07-m) discharging vertically up to 1.2 m^3 in about 10 seconds. The study is focused on the unsteady flow patterns, the discharge capacity and the velocity field in the reservoir. The results are compared with "classical" orifice flow results. The section 2 describes the experimental facility. Section 3 presents the basic results. Section 4 details some specific aspect.

---

[1] That is, clepsydra.

[2] Hero of Alexandria (1st century A.D.) wrote a treaty on water clock in four books.

[3] For example, the egg timer.

[4] Jean-Charles de BORDA (1733-1799) was a French mathematician and military engineer. He achieved the rank of Capitaine de Vaisseau and participated to the U.S. War of Independence with the French Navy. He investigated the flow through orifices and developed the Borda mouthpiece.

[5] This relationship is called Torricelli theorem, after Evangelista TORRICELLI (1608-1647) who discovered it in 1643.

[6] For example, HUNT (1968) for axisymmetrical jets and MISES (1917) for two-dimensional jets. The result for round orifice was proposed first by E. TREFFTZ. For two-dimensional jets, $C_c = \pi/(\pi+2)$. This results was derived independently y JOUKOWSKI and MICHELL in 1890 (JOUKOWSKI 1890, MICHELL 1890).

Fig. 1-1 - Clepsydra (water clock)

(A) Sketch

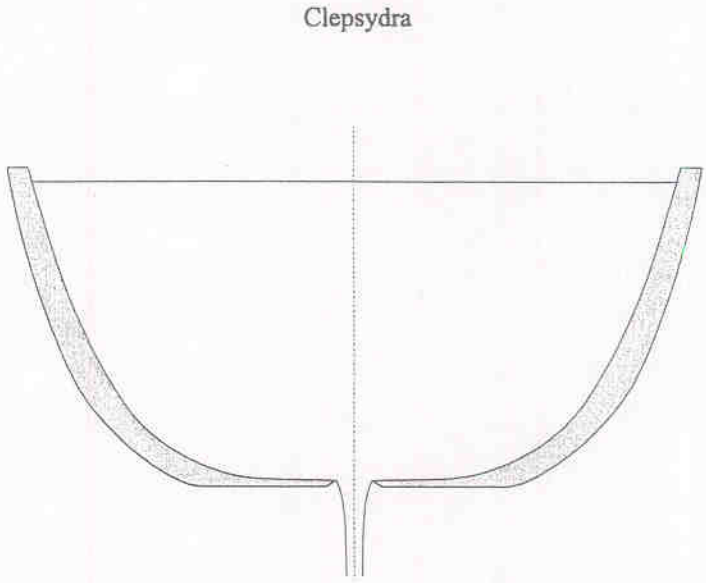

(B) Section shape of a clepsydra : orifice diameter: 4 mm, emptying time: 23 hours

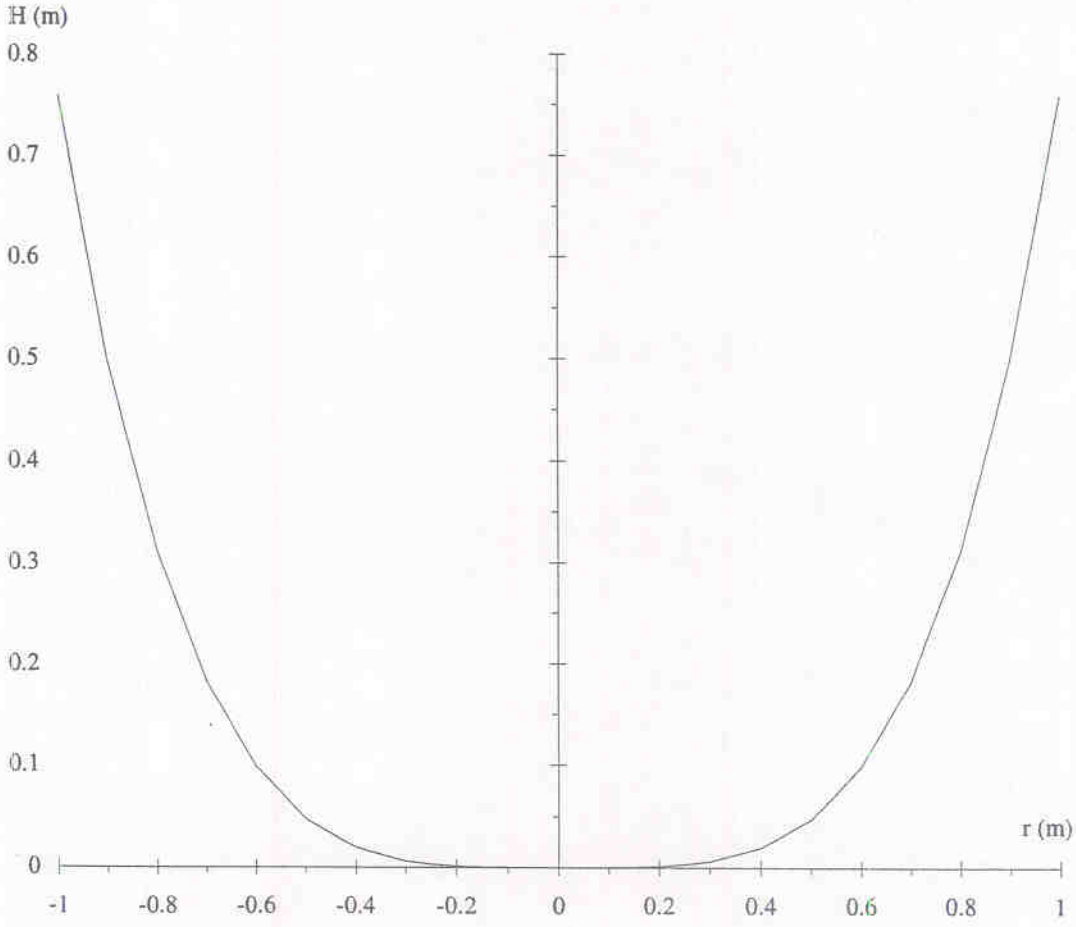

2. EXPERIMENTAL CONFIGURATION

New experiments were performed with a rectangular sharp-edge orifice (0.750-m by 0.070-m) made from a 10-mm thick perspex sheet and located at the bottom of a circular water tank, 0.8-m high with internal diameter ranging from 1.3 m at the base up to 1.35-m at the top (Fig. 2-1 and 2-2). The orifice was closed by a 4.1-kg steel gate (0.11 m*0.79 m*0.006 m). Two L-shaped stiffners were added inside the tank and located parallel to the orifice. Their upper edge was 41-mm above the orifice and they were placed 143-mm apart from the orifice centreline. Flow visualisations suggested that the stiffners had little effect on the orifice flow for head above orifice larger than 0.1-m.

The relationship between the water elevation above orifice edge and water volume was measured in-situ with a calibrated 40-L container :

$$\text{Volume} = 1.3889 * (H + 0.01)^{1.035455} \qquad (2\text{-}1)$$

where H is the total head above orifice edge, with a normalised correlation coefficient of 0.999989. During the experiments, the orifice flow discharged vertically into a large container located at least 1.5-m beneath the orifice.

Time origin and system of references

Gate opening resulted from unlatching three pins with a hammer. High-speed video pictures demonstrated that the unlatching occurred in less than 30 milliseconds and the full opening of the gate took about 180 to 230 milliseconds.

The time origin (t=0) is taken at the time of impact of the hammer on the pins. The origin of the system of coordinates {x, y, z} is taken at the centre of the orifice with z positive upwards, x along the short orifice centreline and y along the long centreline.

Instrumentation

Flow visualisations and the nappe trajectory were investigated with two video-cameras : a VHS-C camescope National™ CCD AG-30C (speed: 30 frames/sec., shutter: 1/60 & 1/1,000 sec.) and a digital handycam Sony™ DV-CCD DCR-TRV900 (speed: 30 frames/sec., shutter: 1/4 to 1/10,000 sec., zoom: 1 to 48).

Water depths in the water tank were measured with pointer gauges and a 0.8-m long capacitance wave gauge. The wave gauge has a 10-Hz response and an accuracy of about 1 mm that was tested during on-site calibration with the pointer gauges. It was calibrated (each day) by comparing the voltage output with point gauge readings for a range of water heights, and calibration curves were best-fitted to the readings.

Velocity measurements were performed with a 3-D acoustic Doppler velocimeter (ADV) Nortek™ ADVLab equipped with a 5-cm downlooking sensor ([1]) mounted on a rigid 40-cm stem (Fig. 2-3). The system was calibrated in factory and it should not need re-calibration. The accuracy on the velocity was expected to be about 0.025 m/s ([2]) but larger errors were experienced close to the orifice because of the size of the sampling volume.

---

[1]On-site measurements showed that the exact distance from the sampling volume to the probe tip was 55-mm.

[2]The manufacturer specifies a 1% full-scale accuracy.

The latter was approximately 6-mm in diameter (Nortek 1996). This dimension is basically the error on the ADV sampling volume position. The accuracy of the ADV velocity was supposed to equal the velocity difference across the sampling volume (see below).

The ADV system was oriented in the yz-plane with a 40- to 60-degrees angle to the horizontal to avoid wake interference caused by the probe tip into the sampling volume ([3]). The three velocity components were reconstructed by a rotation around the Ox axis.

ADV-velocity data: noise

It should be noted the high level of noise observed in the 3 velocity component signals. At rest, the measured ADV signal represents the Doppler noise itself. Once the orifice gate is open, the "measured" (?) velocity fluctuations characterise the combined effects of the Doppler noise, velocity fluctuations and installation vibrations. It is acknowledged that the Doppler noise level increases with increasing velocity although it remains of the same order of magnitude as the Doppler noise at rest. NIKORA and GORING (1998) and more specifically LEMMIN and LHERMITTE (1999) discussed in details the inherent noise of an ADV system.

No turbulence measurement could be performed accurately during the study because the Doppler noise was of the same order of magnitude as (if not larger than) true turbulent velocity fluctuations ([4]).

---

[3]Flow visualisations confirmed the absence of interference from the probe transducers on the sampling volume.

[4]For completeness, a later study using this particular ADV device found some problem with the device which had to be sent back to the manufacturer.

Fig. 2-1 - Sketch of the experiment

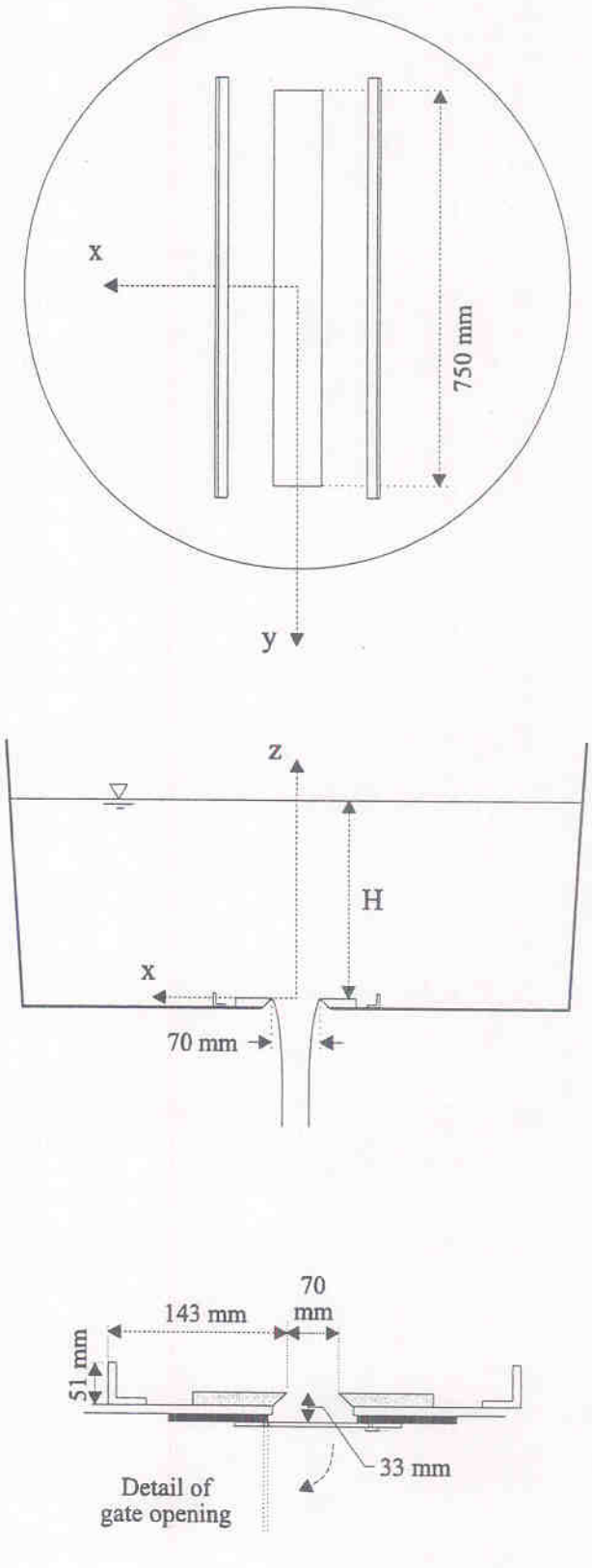

Fig. 2-2 - Photographs of the experimental apparatus

(A) Inside of the water reservoir

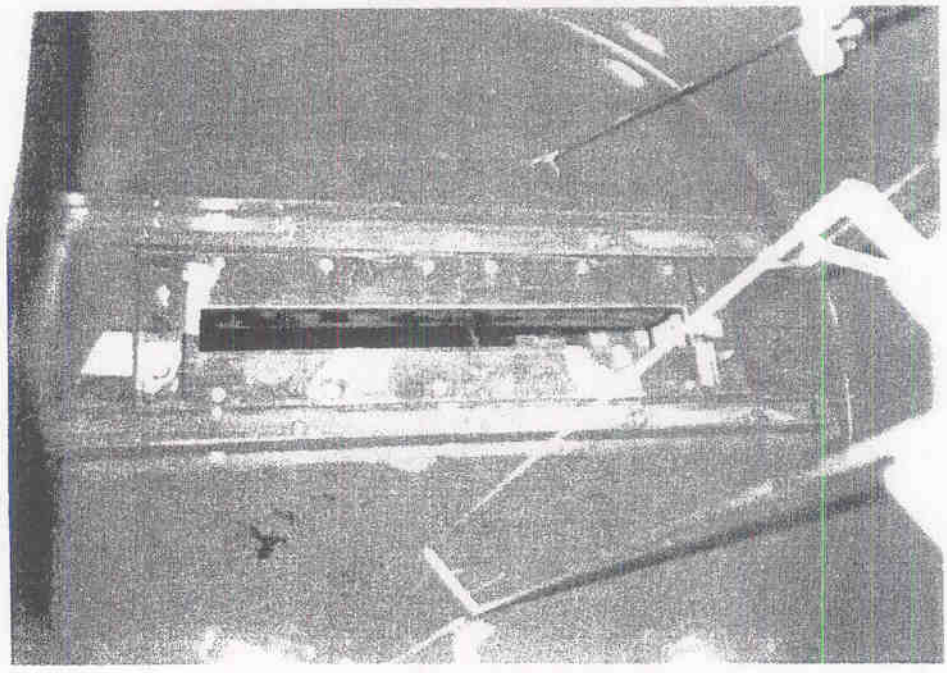

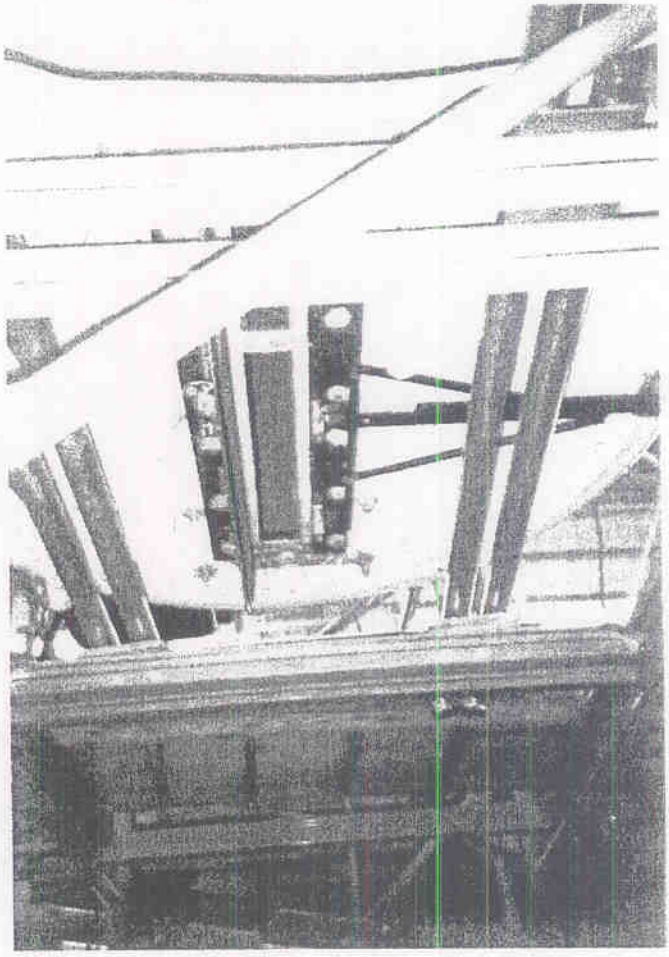

(B) Details of the gate fully-opened

Fig. 2-3 - Photographs of the ADV system

(A) Run 990331b : prior to gate opening

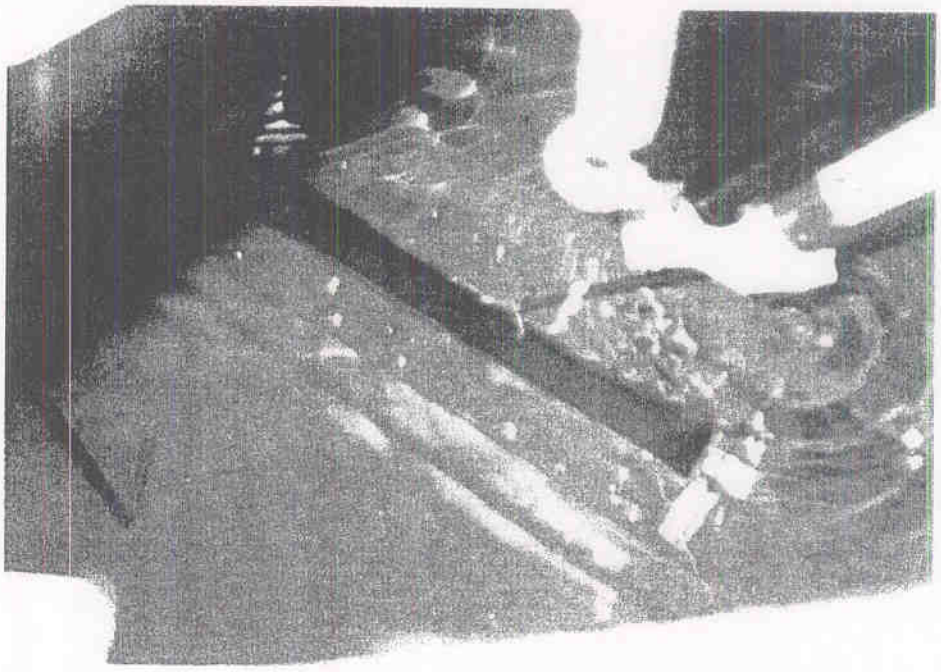

(B) Run 990331b : after gate opening during orifice flow

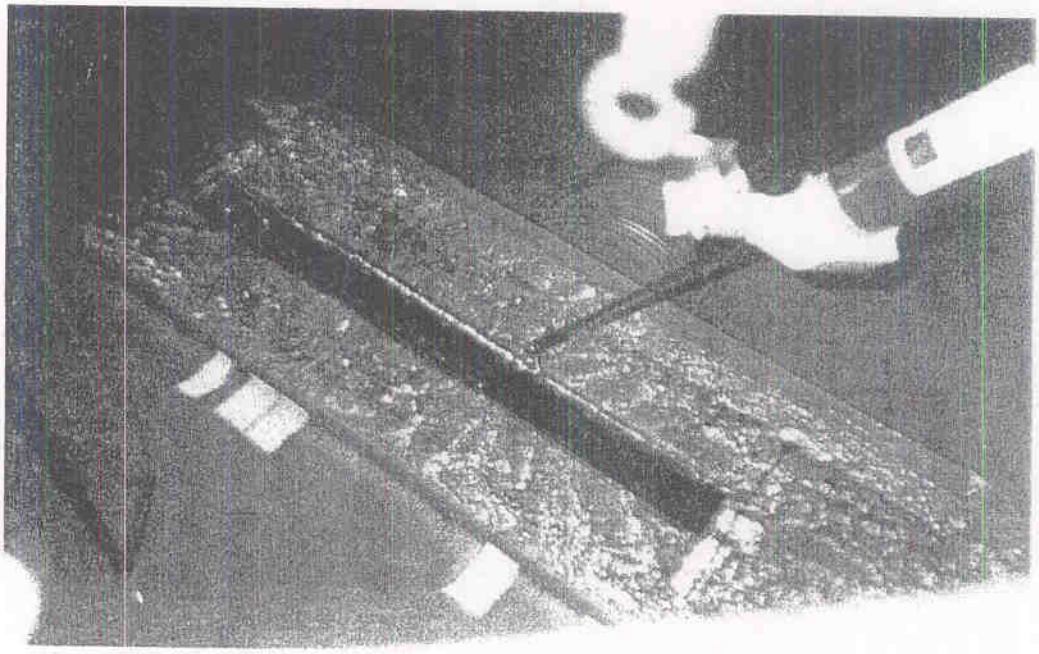

3. EXPERIMENTAL RESULTS

3.1 Unsteady flow patterns

The unsteady flow pattern resulting from the gate opening is characterised by an initial phase with rapid aeration of the water next to the orifice (mixing flow), a flow acceleration phase associated with free-jet expansion downstream of the orifice (bursting flow), a quasi-steady flow period and, near the end, a free-surface flow over the orifice edges (Table 3-1, Fig. 3-1 to 3-6). Overall the discharge duration was about 10 seconds for an initial water volume of one thousand litres. Photographs of the orifice flow are shown in Figure 3-1 and 3-2.

Table 3-1 - Unsteady orifice flow patterns

t (1)	Flow pattern (2)
$0 \Rightarrow$ 68 to 133 ms	Mixing flow
67 to 133 ms $\Rightarrow$ 150 to 230 ms	Bursting flow
150 to 230 ms $\Rightarrow$ $H/b_o > 0.5$	Quasi-steady flow
$H/b_o < 0.43$ to 0.5	Free-surface flow (weir overflow)

Notes: b_o : short orifice dimension; H : head above orifice.

Fig. 3-1 - Photographs of the experiment

(A) Gate opening (H_1 = 0.653 m, t ~ 0.06 s) - Gate hinge on the left

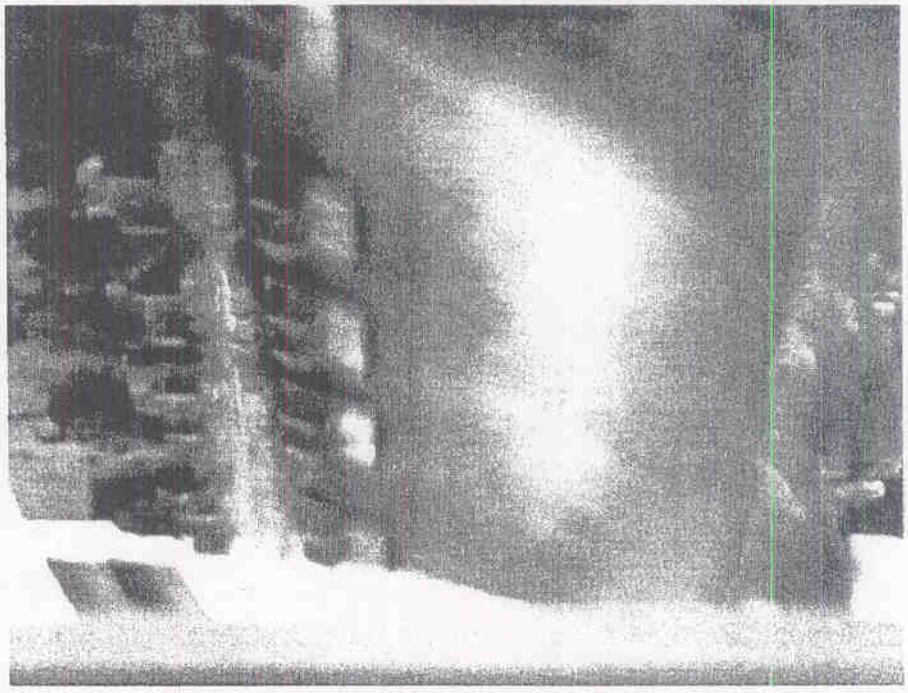

(B) Bursting flow ($t < 0.22$ s) - Experiment 990413_5 : $H_1 = 0.650$ m (water volume: 0.903 m^3)

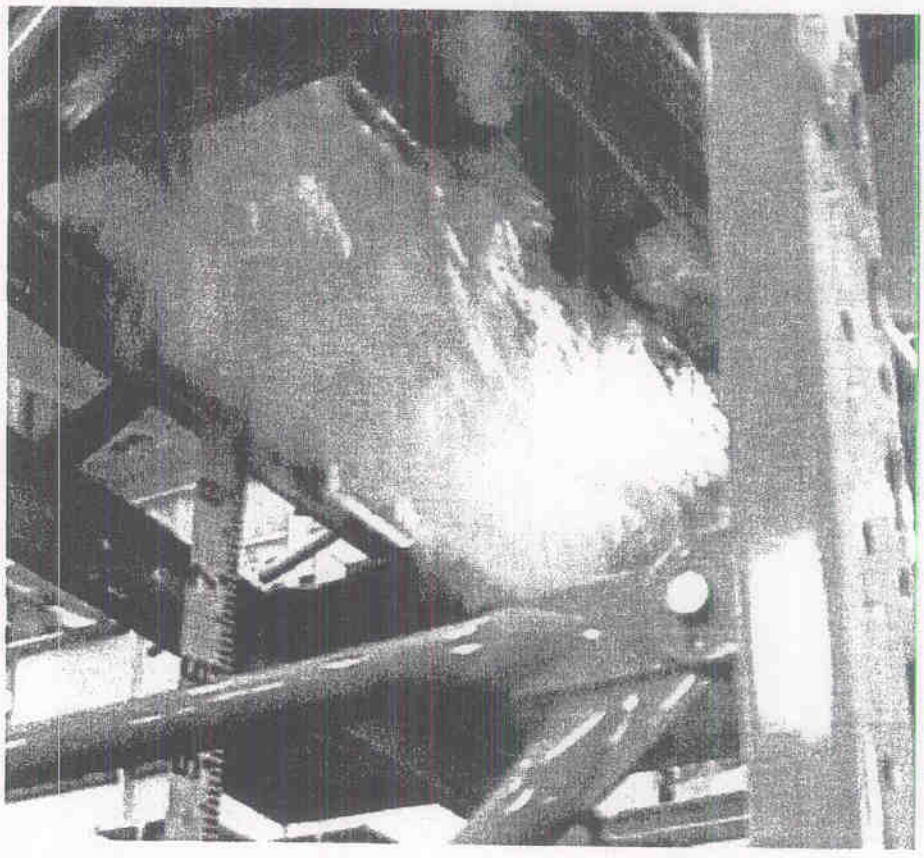

(C) Sideview of the free-falling jet (Test 990301a) during calibration tests

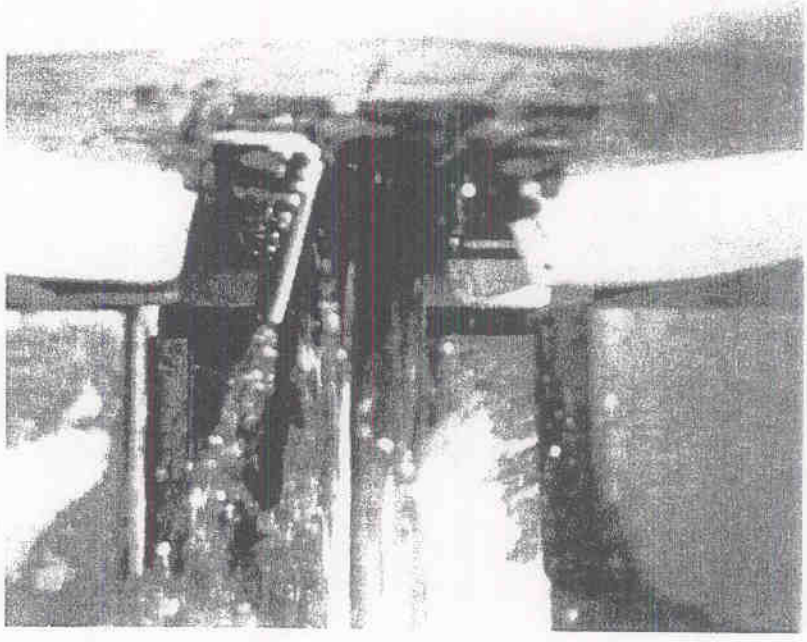

Fig. 3-2 - Typical orifice flow sequences (A) Free-falling nappe - Front view (H_1 = 0.653 m)

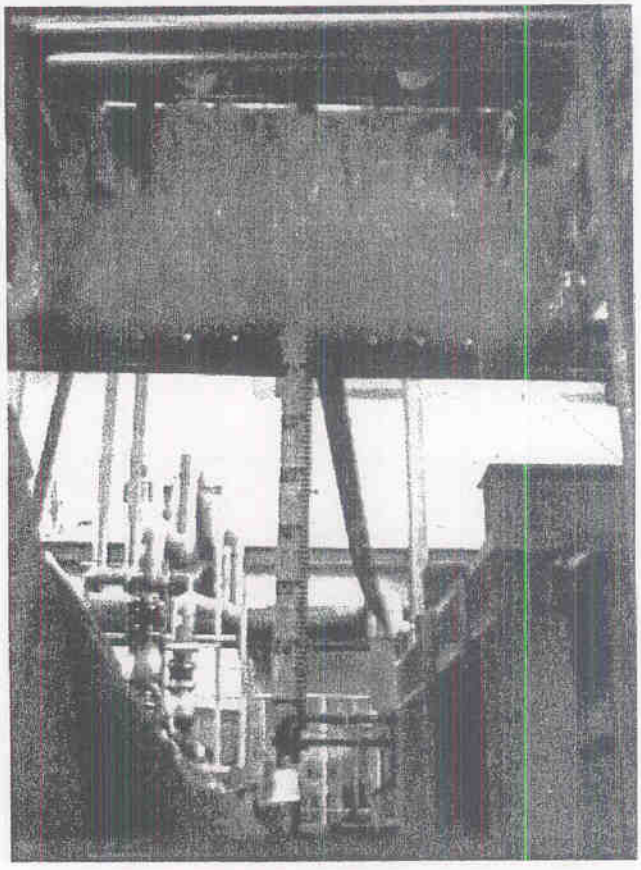

(A1) Initial bursting flow

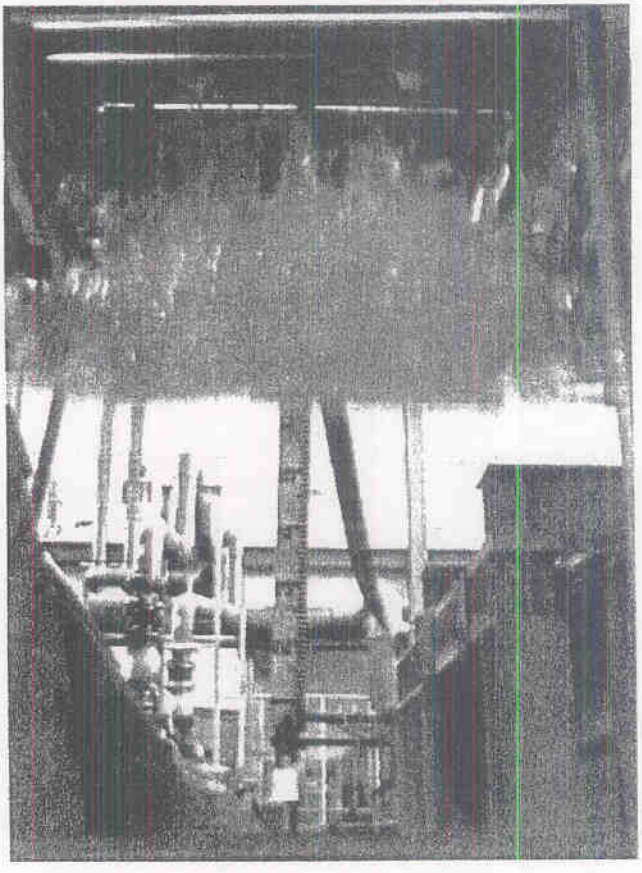

(A2) Bursting flow

Fig. 3-2 - Typical orifice flow sequences

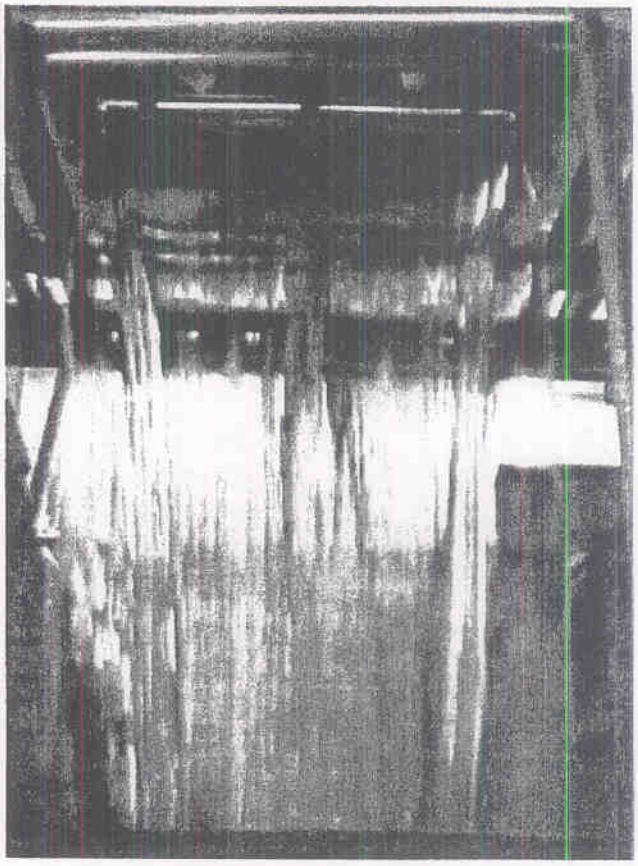

(A3) Quasi-steady flow

(B) Free-falling nappe - Sideview (H_1 = 0.652 m)

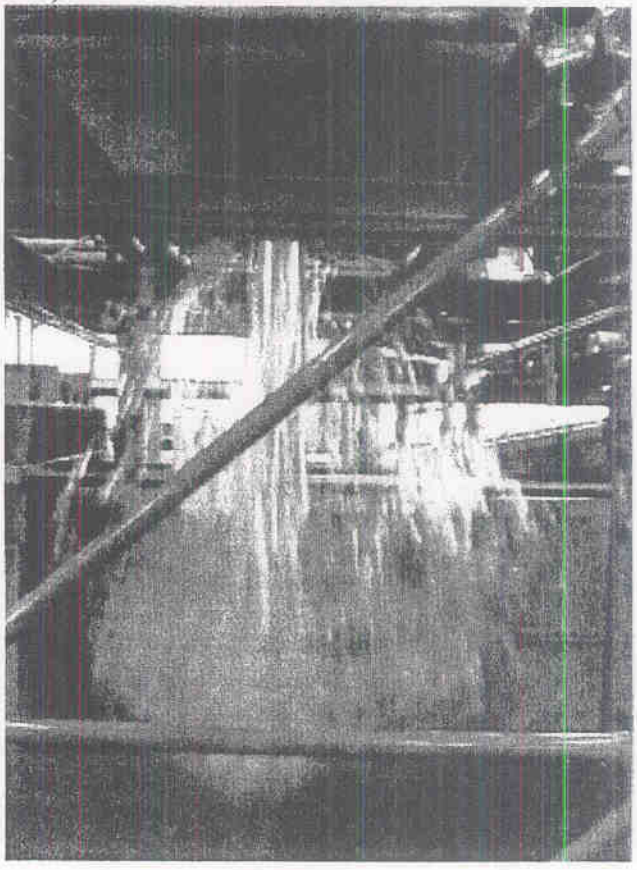

(B1) Bursting flow

Fig. 3-2 - Typical orifice flow sequences

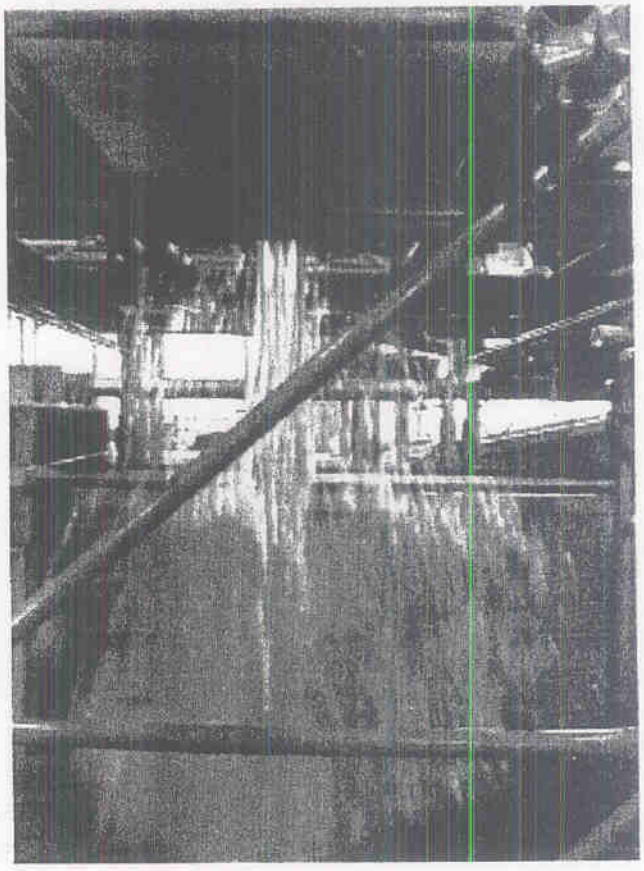

(B2) End of bursting flow

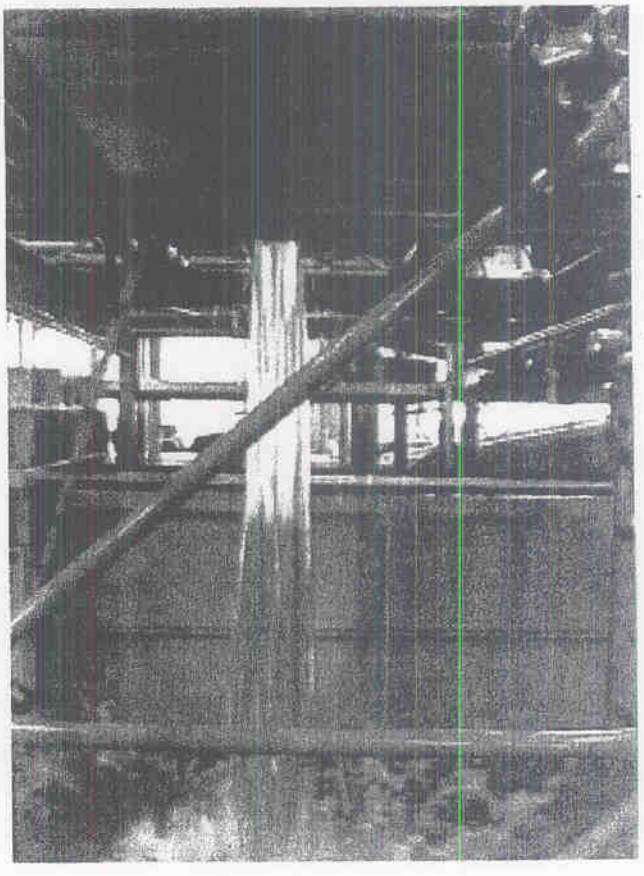

(B3) Quasi-steady flow

Fig. 3-3 - Sketch of the mixing flow pattern

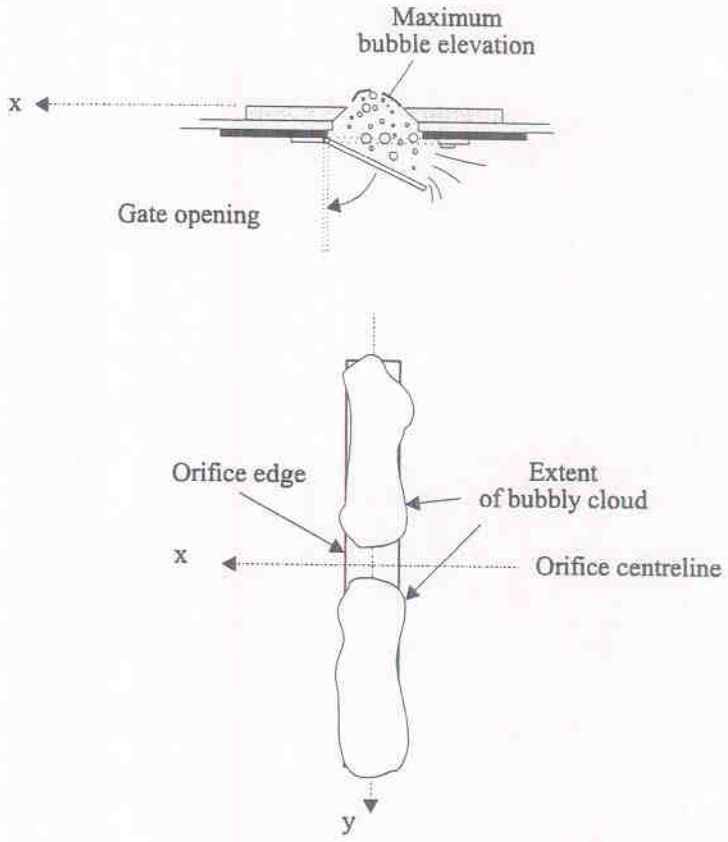

Mixing flow / Multiphase flow

In the initial instants following the gate unlatching, the hydrostatic pressure force acting on the gate adds to the weight of the gate and contributes to a rapid gate opening. However the jet flow starts slowly and accelerates with time t.

Visual observations with an underwater camera (located inside the reservoir) showed that some air tends to flow upwards into the reservoir up to and slightly above the orifice edge for $t > 0$. The duration of this mixing phase is about 67 to 133 ms (2/30 to 4/30 s). The air bubbles are observed to enter all around the gate, although the bubbly flow region is not two-dimensional (Fig. 3-3). Little air is observed near the orifice centreline (i.e. $y = 0$). The maximum elevation reached by the air was about 5 to 10 mm above orifice edge. Afterwards the air was entrained downwards by the jet flow. The flow pattern was observed consistently for $0.3 < H_1 < 0.75$ m and $t <$ 67 to 133 ms.

The gate opening is somewhat analogous to a negative surge at a penstock forebay ([1]). Considering an open channel supplying a hydropower plant, the sudden start of the plant creates a negative wave in the forebay channel. The disturbance (i.e. negative wave) propagates with a speed $C = \sqrt{g*H_1}$ ([2]). By analogy, the

---

[1]For example, HENDERSON (1966), pp. 322-324, MONTES (1998), pp. 487-489.

[2]In a particular case, experimental observations showed that the celerity of the negative surge was $2*\sqrt{g*H_1}$ (LAUBER and HAGER 1998).

disturbance created by the sudden orifice opening would reach the free-surface at $t = H_1/C = 257$ ms for $H_1 = 0.65$ m, , that is a time scale similar to the duration of the mixing flow.

Remark

For completeness, another analogy could be the surge tank. The circular tank is somehow analogous to a 1.3-m diameter fibreglass pipe in which the wave celerity is about C ~ 300 m/s ([3]). The time period of pressure oscillations in the tank is $4*H_1/C = 8.7$ ms for $H_1 = 0.65$ m. Such a time frame is one to two orders of magnitude smaller than the duration of the mixing flow.

Bursting jet / Accelerating flow

Once the reservoir water accelerate, the jet flow bursts downwards out of the orifice (Fig. 3-4). The leading edge of the jet is preceded by aerated waters spreading in both the x- and y-directions (i.e. "bursting flow"). Experimental observations indicate that the lateral spread angles of the jet θ_x and θ_y are nearly independent of the initial total head : i.e., $\theta_x = 33$ to 55 degrees and $\theta_y \sim 15$ degrees for $0.3 < H_1 < 0.75$ m. The "bursting flow" lasts up to t = 150 to 230 ms at the orifice.

It was initially thought that the "bursting flow" was caused by the sudden expansion of the water volume located between the gate and the orifice (i.e. - 33 mm < z < 0) (Fig. 2-1, bottom). It is now believed that the flow pattern results from the sudden expansion of the air-water mixture generated during the initial instants (i.e. mixing flow phase).

Note that, for very-small circular jets discharging vertically from a cylinder, the leading edge of the jet was observed to have a round bulging shape (STORR and BEHNIA 1999). It is likely that surface tension prevented the aeration of the jet edges.

Fig. 3-4 - Sketch of the "bursting flow" pattern

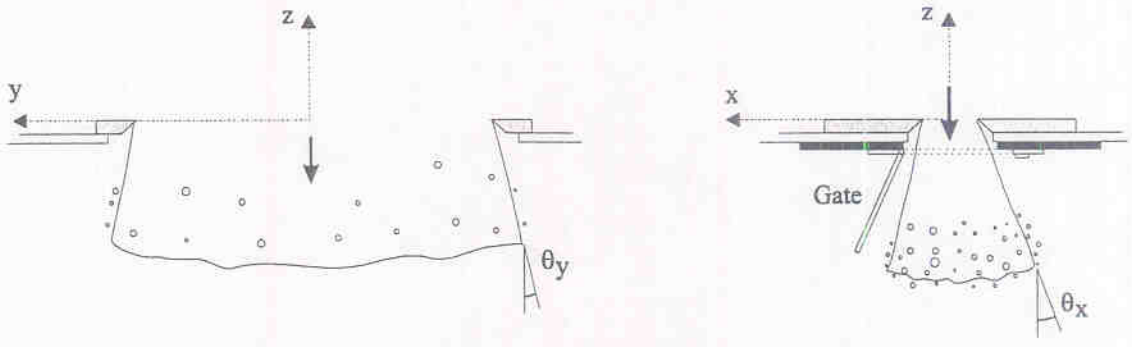

[3]The wave velocity for pressure waves is about 300 to 400 m/s in PVC pipes, 1,000 m/s in ductile iron pipes, and abou 1,450 m/s in rigid pipes.

Quasi-steady flow

After the establishment of the jet flow, the flow pattern becomes quasi-steady. Nappe contraction is observed downstream of the orifice. The observed nappe contraction b/b_o is best correlated by :

$$\frac{b}{b_o} = 0.94 - 0.021 * \frac{H_1}{b_o} \qquad \text{for } 5 < H/b_o < 11 \quad (3\text{-}1)$$

where b is the free-falling nappe thickness observed at $z/b_o \sim -1$ (Fig. 3-5).

The nappe contraction in the y-direction was observed to be: $B/B_o \approx 0.8$ to 0.85. For rectangular sharp-crested weirs with side contractions, the lateral contraction of the overflow nappe is about 0.8 (e.g. ACKERS et al. 1978, pp. 59-61).

Dye injection in the tank associated with underwater video-pictures confirmed the smooth flow contraction into the orifice. No dye mixing was observed anywhere anytime in the reservoir. The observation was valid everywhere including around the ADV sensors.

Fig. 3-5 - Contraction coefficient of the free-falling nappe

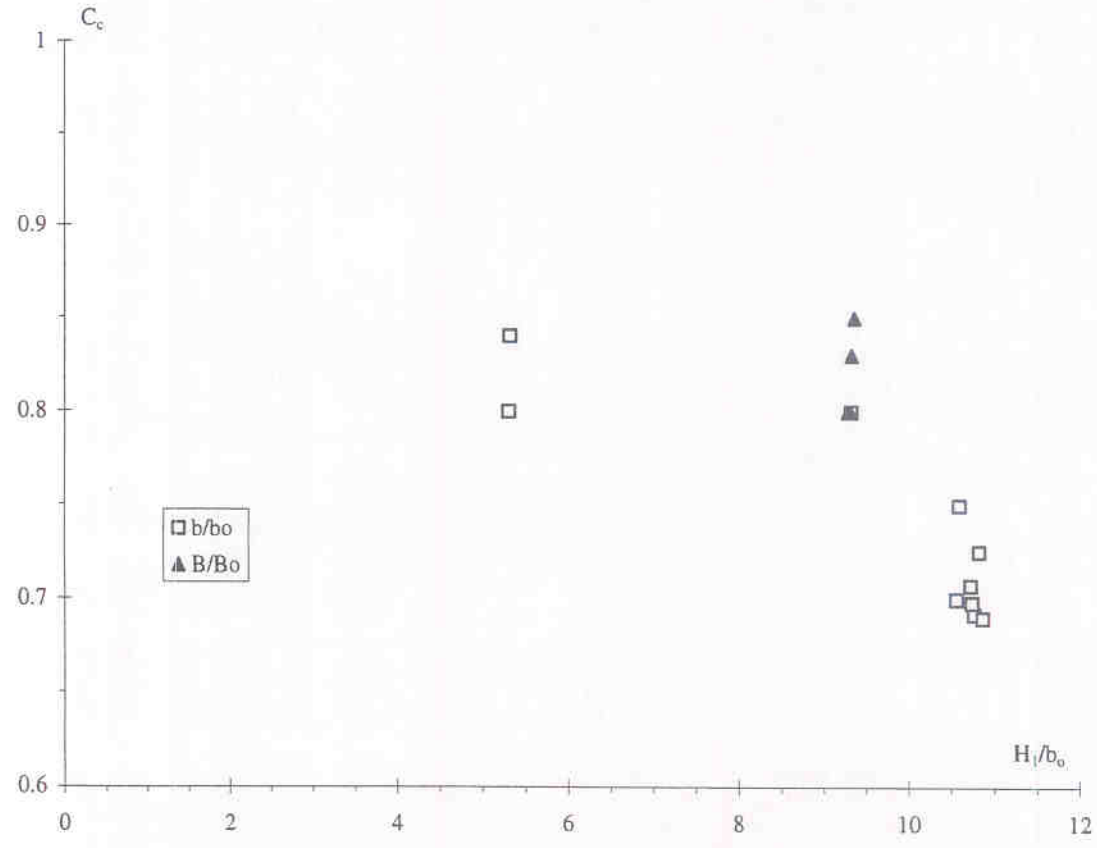

Free-surface overflow / weir overflow

Near the end, the orifice becomes a weir. That is, the flow changes from a submerged flow to a free-surface overflow (Fig. 3-6). Video observations suggest that the orifice flow becomes a free-surface flow for $H/b_o \approx 0.43$ to 0.51.

Fig. 3-6 - Free-surface flow : weir overflow

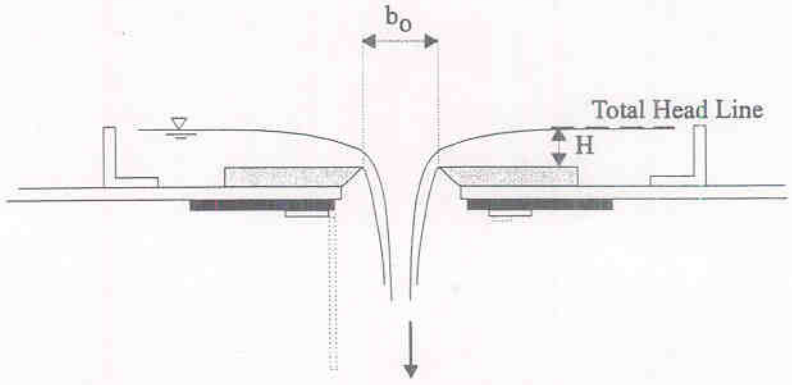

3.2 Orifice discharge coefficient

For a horizontal jet discharging through a two-dimensional orifice, the flow rate equals :

$$Q = C_D * B_o * b_o * \sqrt{2 * g * H} \qquad (3\text{-}2)$$

where B_o and b_o are the orifice dimensions and C_D is a discharge coefficient that takes into account the nappe contraction downstream of the orifice and the energy losses.

Assuming that the reservoir free-surface area A is far greater than the orifice area (i.e. $A >> B_o * b_o$), the reservoir surface drops slowly enough and the Bernoulli principle (i.e. Eq. (3-2)) may be applied with a small error. The continuity equation for an incompressible fluid states that the outflow equals the change of reservoir volume :

$$Q * \Delta t = - A * \Delta H \qquad (3\text{-}3)$$

where Δt is a small time interval. Combining Equations (3-2) and (3-3), and integrating between $H = H_1$ at $t = t_1$ and $H = H_2$ at $t = t_2$, it yields :

$$t_2 - t_1 = \frac{-1}{\sqrt{2*g} * B_o * b_o} * \int_{H_1}^{H_2} \frac{A}{C_D * \sqrt{H}} * dH \qquad (3\text{-}4)$$

A further assumption is that C_D is nearly constant :

$$t_2 - t_1 = \frac{-1}{\sqrt{2*g} * C_D * B_o * b_o} * \int_{H_1}^{H_2} \frac{A}{\sqrt{H}} * dH \qquad (3\text{-}5)$$

During the present series of experiments, C_D was found to be independent of time ([4]) provided that $H > 0.1$ to 0.15 m. The discharge coefficient C_D was found to be between 0.62 and 0.65. This value is larger than ideal-fluid flow theory and data for orifice flow discharging horizontally: $C_D = 0.60$ (e.g. TROSKOLANSKI 1960). For an orifice flow discharging vertically, the fluid is accelerated between the orifice and the vena contracta. Equation (3-5) does not account for the difference in elevation between the orifice and the vena contracta. Video

[4] That is, constant for a given experiment.

pictures suggest that a "pseudo-vena contracta" occurs at about $z \approx -1.0*b_o$ ([5]). Equations (3-2) and (3-5) may be corrected accordingly:

$$Q = C_D' * B_o * b_o * \sqrt{2 * g * (H + 1.0*b_o)} \qquad (3\text{-}2b)$$

$$t_2 - t_1 = \frac{-1}{\sqrt{2*g} * C_D' * B_o * b_o} * \int_{H_1}^{H_2} \frac{A}{\sqrt{H + 1.0*b_o}} * dH \qquad (3\text{-}5b)$$

Using Equation (3-5b), the corrected discharge coefficient C_D' was found to be correlated to the initial head above orifice as :

$$C_D' = 0.5832 * \left(1 - \exp\left(-0.6597 * \frac{H_1}{b_o}\right)\right) \qquad (3\text{-}6)$$

where H_1 is the initial upstream head above orifice and b_o is the orifice width. The results are presented in Figure 3-7. They are consistent with the observed nappe contraction (i.e. $b/b_o \approx 0.7$ to 0.85, $B/B_o \approx 0.8$ to 0.85) implying an average contraction coefficient of about $C_c = A/A_o \approx 0.60$. For large head above orifice, the data yield $C_D' \approx 0.58$, a result close to ideal fluid flow results (i.e. $C_c = 0.61$, MISES 1917).

Fig. 3-7 - Orifice discharge coefficient: experimental data

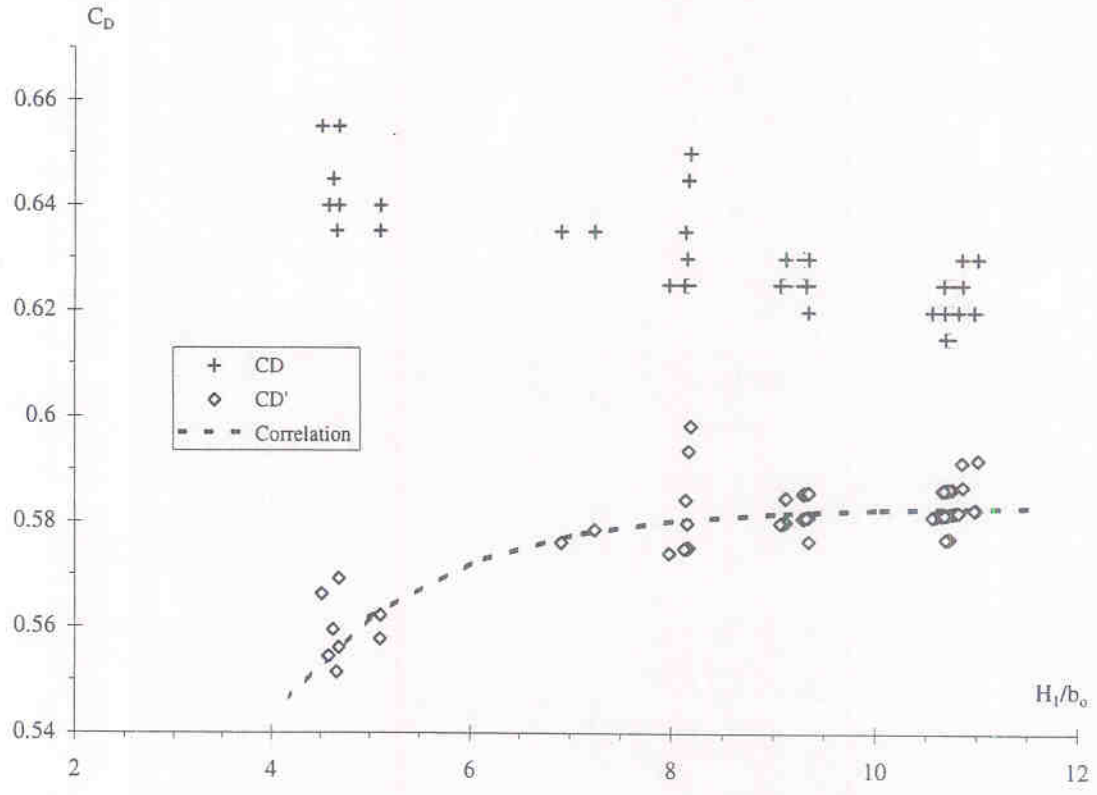

[5]The observation is subjective as the fluid is accelerated. For a horizontal two-dimensional orifice, the vena contracta is observed about 1.7 times the orifice height downstream of the orifice (e.g. MONTES 1998, pp. 283-284).

Remark

For completeness, the writers wish to highlight the sensitivity of C_D' to the vertical location of the pseudo-vena contracta. Although the present selection (z/b_o=-1) is subjective, the results are consistent with independent visual observations of the nappe contraction.

3.3 Velocity field

Velocity measurements were performed in the reservoir upstream of the orifice. Typical data are shown in Figures 3-8, 3-9 and 3-10. The data are presented as $V/\sqrt{2*g*H_1}$ versus H/H_1, where V is the velocity component, $\sqrt{2*g*H_1}$ is the ideal-flow velocity at the orifice, H is the instantaneous total head above orifice and H_1 is the initial total head (i.e. $H_1 = H(t=0)$). Each curve corresponds to a fixed sampling volume (i.e. z/b_o constant). Unless indicated the data were recorded on the short orifice centreline (i.e. $y \approx 0$).

Figure 3-8 shows the vertical velocity component data V_z measured on the orifice centreline ($x = 0$). The free-surface velocity is also shown. Firstly note the scatter of the data that is characteristics of the ADV noise (see paragraph 2.). Secondly the results show some fluid acceleration next to and upstream of the orifice : i.e., for $z/b_o < 3.5$ ($z < 0.245$ m). Above, the water velocity is basically equal to the free-surface velocity. Close to the orifice, the velocity magnitude decreases with decreasing total head : i.e., for $1 < z/b_o < 3.5$.

Figure 3-9 presents experimental data recorded above the orifice edge (i.e. $x/b_o = 0.5$). The vertical velocity component data shows the same trend as on the centreline (x=0) (Fig. 3-8(B)). There is however a horizontal velocity component which becomes significant for $z/b_o < 2$ ($z < 0.14$) (Fig. 3-8(A)).

Figure 3-10 shows measurements performed away from the orifice (i.e. $x/b_o = 3.6$). The results indicate that the velocity magnitude is of the same order of magnitude as the free-surface velocity.

Overall the results are in agreement with a two-dimensional flow net analysis (Fig. 3-11 ([6])).

---

[6]Figure drawn with the software 2DFlowPlus version 2.5.

Fig. 3-8 - Unsteady velocity field in the reservoir: $x/b_o = 0$ ($b_o = 0.070$ m) (V_z component)

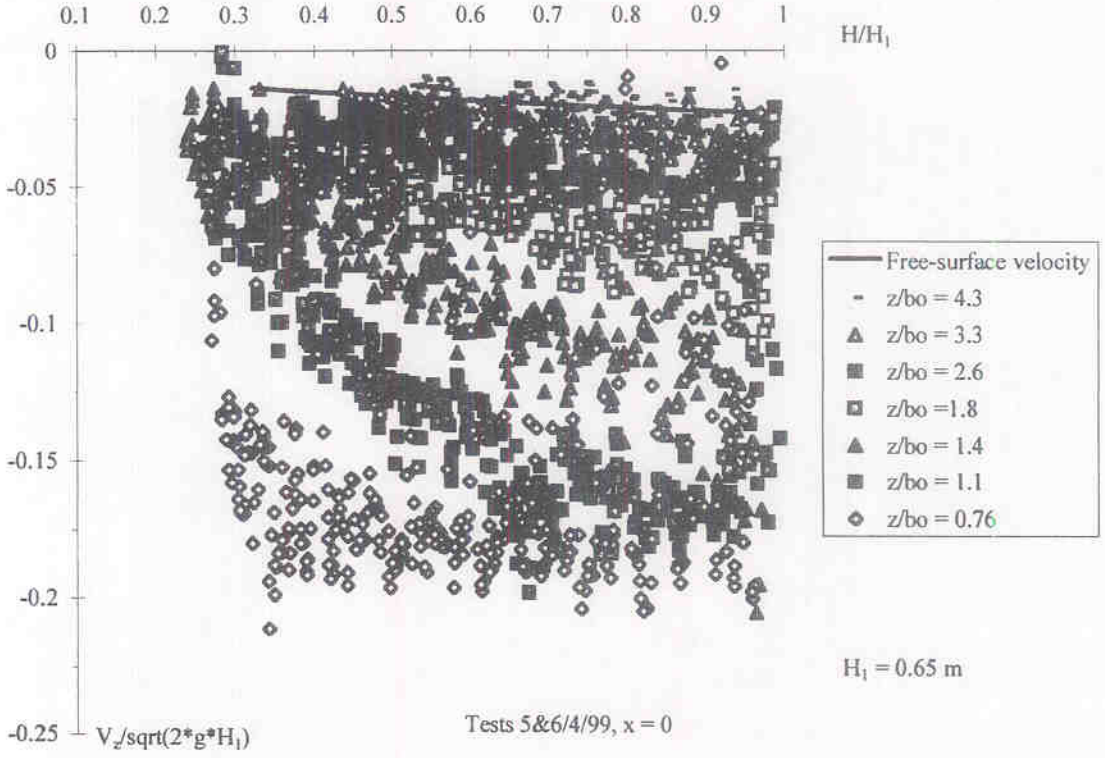

Fig. 3-9 - Unsteady velocity field in the reservoir: $x/b_o = 0.5$ ($b_o = 0.070$ m)

(A) V_x component

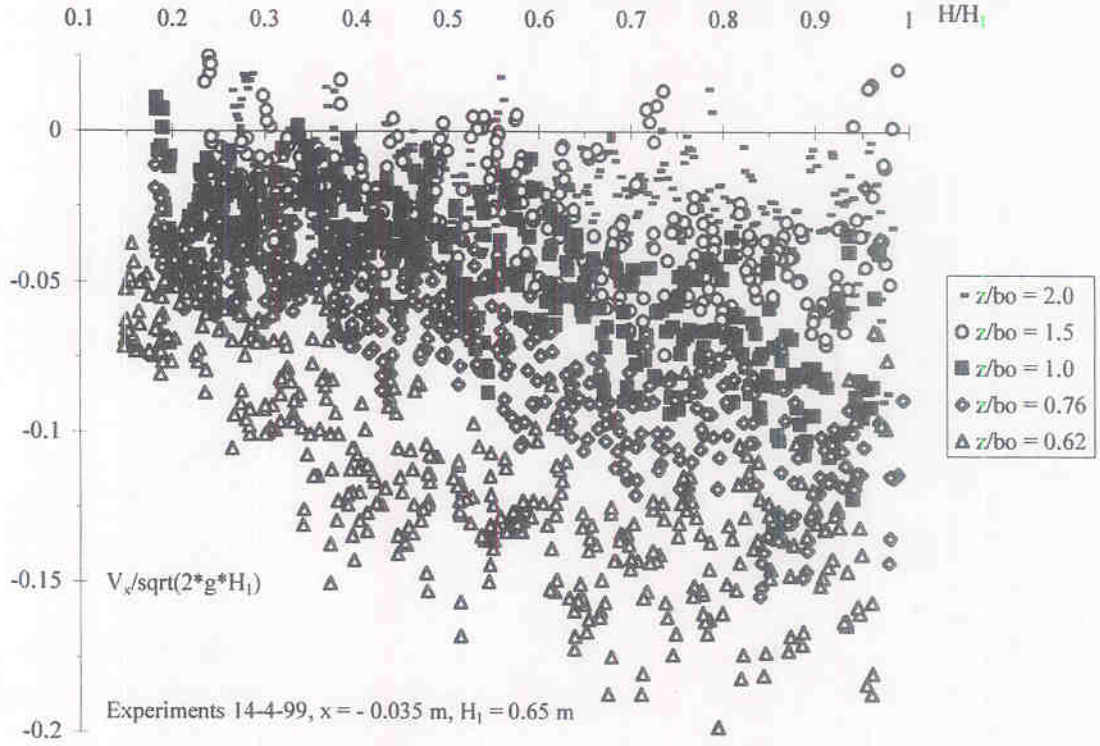

Fig. 3-9 - Unsteady velocity field in the reservoir: $x/b_o = 0.5$ ($b_o = 0.070$ m)

(B) V_z component

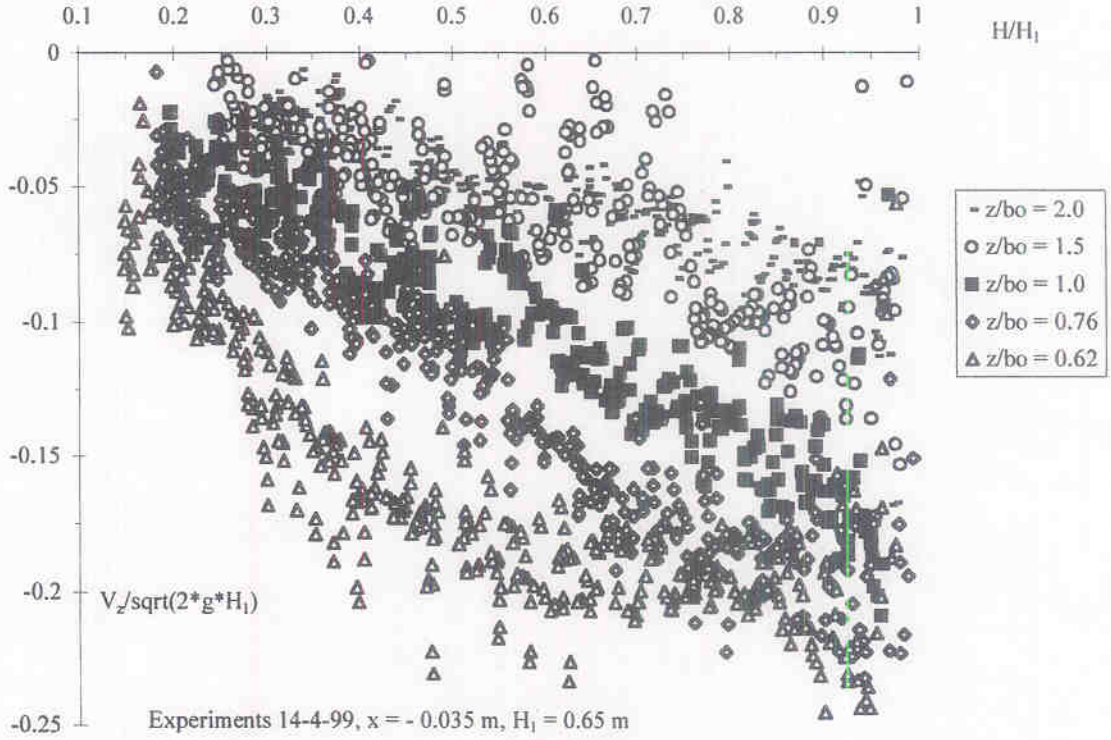

Fig. 3-10 - Unsteady velocity field in the reservoir: $x/b_o = 3.6$ ($b_o = 0.070$ m)

(A) V_x component

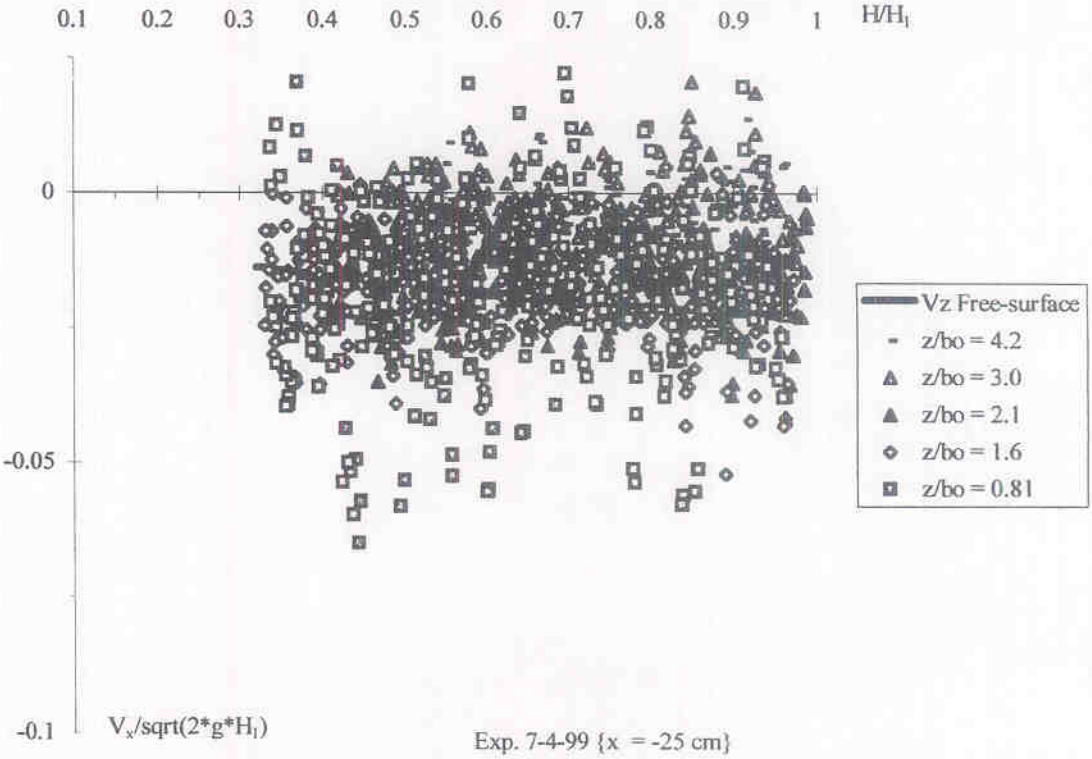

Fig. 3-10 - Unsteady velocity field in the reservoir: $x/b_o = 3.6$ ($b_o = 0.070$ m)

(B) V_Z component

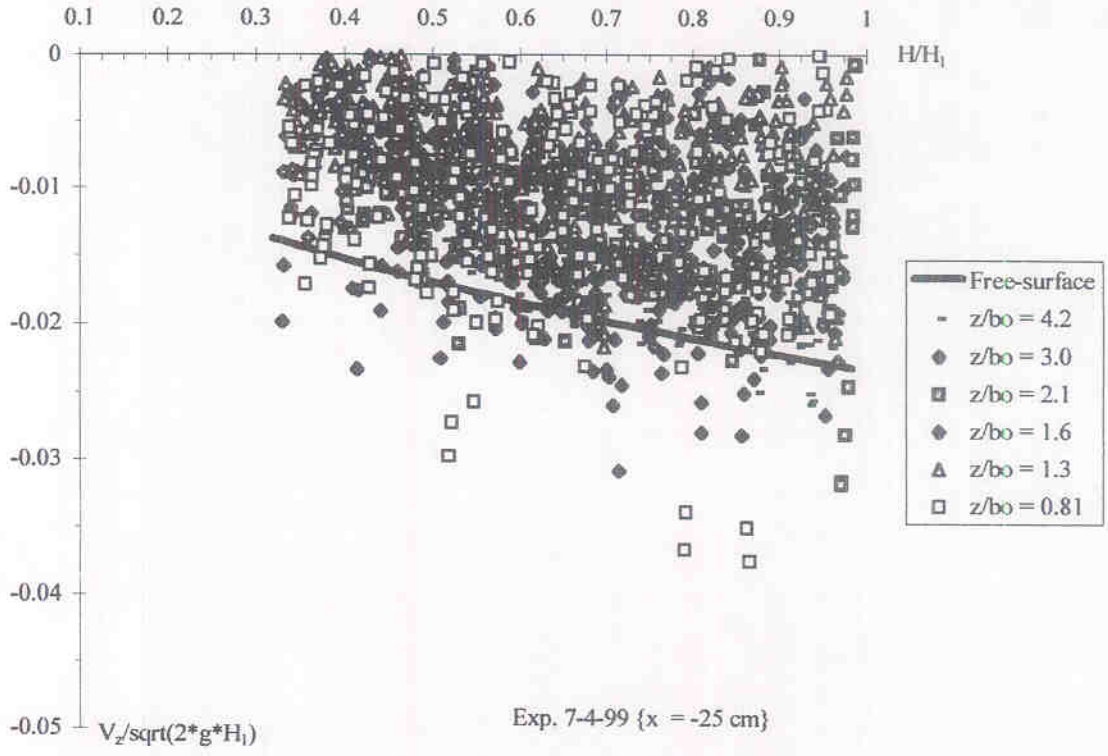

Fig. 3-11 - Two-dimensional flow net

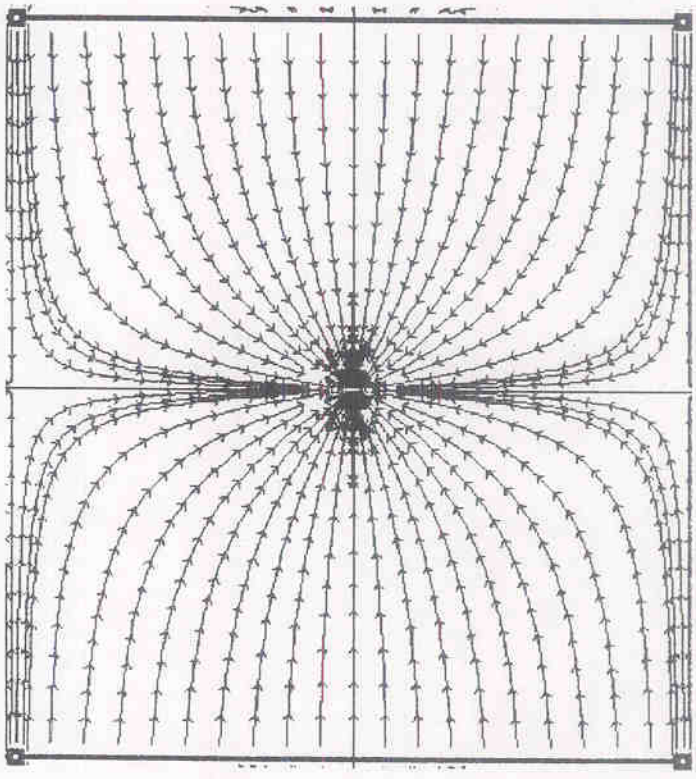

4. DISCUSSION

4.1 Modification of the orifice shape

For one series of experiments, the orifice geometry was modified by inserting some 18-µm thick cellophane sheets between the stiffner edges and the orifice (Fig. 4-1). The cellophane sheets were clipped onto the stiffners with a smooth rounded cover. The sheets were slightly wider than the orifice width (B_o = 0.75 m) and they extended up to 2-m below the orifice. Video-pictures showed that the plastic cellophanes were stretched between the stiffners and the orifice edges and they adhered to the jet interfaces without affecting visually the jet flow, but very close to the outer edges of the free-jet.

Experimental data are presented in Figure 4-2 in terms of both C_D (Eq. (3-2)) and C_D' (Eq. (3-2b)). The results show that the discharge coefficient is increased by 20 to 25% typically with the thin plastic cellophanes. It is believed that the plastic sheets induced three effects: a convergence (δ = 16°) into the orifice, a smoother wall roughness upstream of the orifice edges, and a "smooth-rounding" of the orifice edges.

Several researchers showed that a convergence of the reservoir boundaries increases the discharge coefficient of an orifice (Table 4-1). For irrotational motion of ideal fluid, the contraction coefficient C_c rises from 0.61 to 0.65 for δ = 0° and 16° respectively ([1]). The plastic cellophane sheets created smooth convergent walls. It is expected that lesser energy losses and hence a greater velocity coefficient C_v would occur. Altogether these combined effects does not explain completely the observed values of the discharge coefficient. It is proposed that the plastic cellophanes induce a smooth rounding of the orifice edge which in turn generates a form of Coanda effect leading to a thicker free-jet. That is, the flow streamlines would tend to follow the plastic sheet curvature and a smaller contraction coefficient would be observed.

In summary, the presence of plastic cellophanes lead an increase of discharge capacity that is best correlated by:

$$C_D' = 0.6734 + 0.0083 * \frac{H_1}{b_o} \qquad (4\text{-}1)$$

Fig. 4-1 - Modification of the orifice geometry

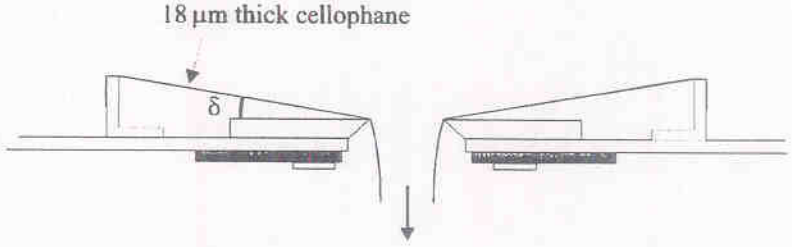

[1] assuming zero gravity and for an infinite reservoir (e.g. MONTES 1997).

Table 4-1 - Effect of convergent on contraction coefficient

Reference (1)	Formulation (2)	Remarks (3)
Irrotational motion of ideal fluid VALLENTINE (1969)	$C_D = \frac{\pi}{\pi + 2}$ for $\delta = 0$ $C_D = \frac{\pi}{\pi + 1.064}$ for $\delta = 45$ degrees	Two-dimensional orifice flow. Ideal-fluid flow theory. Infinite volume.
MONTES (1997) (*)	$C_c = 0.61$ for $\delta = 0$ $C_c = 0.69$ for $\delta = 30$ degrees $C_c = 0.747$ for $\delta = 45$ degrees	Two-dimensional planar gate. Ideal-fluid flow theory. Infinite volume. Numerical integration, inverse method.
	$C_c = \frac{\pi}{\pi + 2 * \int_0^1 \frac{1}{t} * \sin\left(\frac{\pi/2 - \delta}{\pi/2} * \sin^{-1} t\right) * dt}$ (*)	Analytical solution for infinite volume. δ in radians.
	$C_c = 0.611 + 0.132*\delta + 0.0291*\delta^2 + 0.0283*\delta^3$ $0 \le \delta \le 90$ degrees (*)	Correlation (best fit). δ in radians.
Planar gates (sluices) HENDERSON (1966)	$C_c = 1 - 0.75*(1-\delta/(\pi/2)) + 0.36*(1-\delta/(\pi/2))^2$ for $0 < \delta < 90$ degrees	Horizontal sluice gates. δ in radians.
MONTES (1998)	$C_D = 0.46 + 0.54*\exp(-0.8*(\pi/2 - \delta))$	Horizontal sluice gates. Analysis of experimental results by COZZO. δ in radians.

Notes: C_d : contraction coefficient; C_D : discharge coefficient; (*) : re-analysis and correction by the first writer.

Fig. 4-2 - Discharge characteristics of the modified orifice (plastic cellophanes)

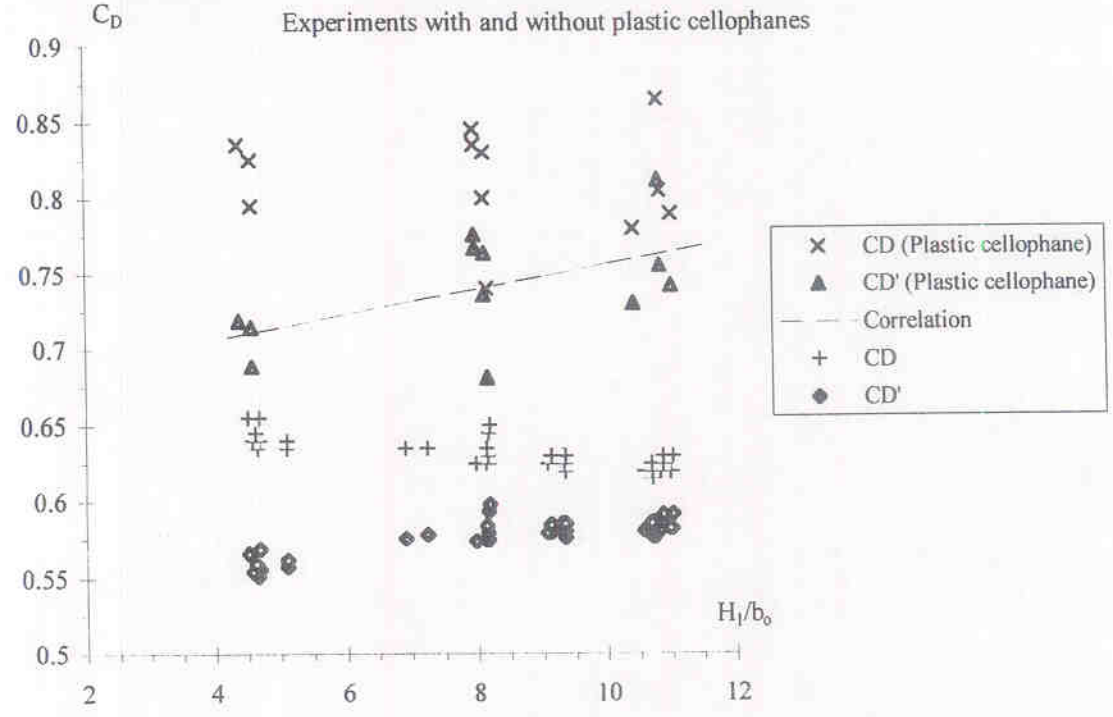

5. SUMMARY AND CONCLUSION

The present study investigates the unsteady pattern of a rectangular orifice flow. The experimental investigation was conducted in a large-size facility with a rectangular orifice (0.75-m by 0.07-m). The orifice flow discharged vertically up to 1.2 m^3 in about 10 seconds.

The results highlight four successive flow patterns (Table 3-1). The gate opening is characterised by an initial phase with rapid aeration of the water next to the orifice (mixing flow), followed by the flow acceleration and free-jet expansion downstream of the orifice (bursting flow), a quasi-steady flow period and, near the end, a free-surface overflow.

The quantitative characteristics of each phase were developed (paragraph 3.1). The discharge coefficient of the vertical orifice flow was found to be very close to that of horizontal orifice flows, although a correction had to account for the vertical jet geometry (paragraph 3.2). Larger discharge coefficient results were obtained with a converging orifice (paragraph 4.1).

The unsteady velocity field is consistent with potential flow calculations, although the latter were developed for steady flow. Some fluid acceleration is observed next to and upstream of the orifice (i.e. for $z/b_o < 3.5$) while elsewhere the vertical velocity nearly equals the free-surface velocity.

Further investigations are required to gain a better understanding of the velocity field in the initial phases (mixing and bursting flow). High-speed data acquisition coupled to a high-speed resolution velocitymeter would be needed.

ACKNOWLEDGMENTS

The authors acknowledge the support of Professor S. NAKAMURA, Department of Architecture and Civil Engineering, Toyohashi University of Technology (Japan). During the first part of the project, the first author was supported by a bilateral fellowship sponsored by the Japan Society of the Promotion of Science and the Australian Academy of Science.

REFERENCES

ACKERS, P., WHITE, W.R., PERKINS, J.A., and HARRISON, A.J.M. (1978). "Weirs and Flumes for Flow Measurement." *John Wiley*, Chichester, UK, 327 pages.

HENDERSON, F.M. (1966). "Open Channel Flow." *MacMillan Company*, New York, USA.

HUNT, B. (1968). "Numerical Solution of an Integral Equation for Flow from a Circular Orifice." *Jl of Fluid Mech.*, Vol. 31, Part 2, pp. 361-177.

JOUKOWSKI, N.E. (1890). "Modification of Kirchoff's Method for Determining the Two Dimensional Motion of a Fluid at a Prescribed Constant Velocity on a Given Streamline." *Proc. Math. Symp.*, Moscow, Russia, Vol. XV.

LAUBER, G., and HAGER, W.H. (1998). "Experiments to Dambreak Wave: Horizontal Channel." *Jl of Hyd. Res.*, IAHR, Vol. 36, No. 3, pp. 291-307.

LEMMIN, U., and LHERMITTE, R. (1999). "ADV Measurements of Turbulence: can we Improve their Interpretation ? Discussion" *Jl of Hyd. Engrg.*, ASCE, Vol. 125, No. 6, pp. 987-988.

MICHELL, J.H. (1890). "On the Theory of Free Streamlines." Phil. Trans. Roy. Soc., London, Part A, Vol. 181, pp.389-431.

MISES, R. von (1917). "Berechnung von Ausfluss und Uberfallzahlen." *Z. ver. Deuts. Ing.*, Vol. 61, p. 447 (in German).

MONTES, J.S. (1997). "Irrotational Flow and Real Fluid Effects Under Planar Sluice Gates." *Jl of Hyd. Engrg.*, ASCE, Vol. 123, No. 3, pp. 219-232. Discussion: Vol. 125, No. 2, pp. 208-213.

MONTES, J.S. (1998). "Hydraulics of Open Channel Flow." *ASCE Press*, New-York, USA, 697 pages.

NIKORA, V.I., and GORING, D.G. (1998). "ADV Measurements of Turbulence: can we Improve their Interpretation ?" *Jl of Hyd. Engrg.*, ASCE, Vol. 124, No. 6, pp. 630-634. Discusion: Vol. 125, No. 9, pp. 987-988.

Nortek (1996). "10 MHz ADV Precise Measurements of 3-D Fluid Flow." Nortek AS, Norway, October.

STORR, G.J., and BEHNIA, M. (1999). "Experiments with Large Diameter Gravity Driven Impacting Liquid Jets." *Experiments in Fluids*, Vol. 27, pp. 60-69.

TROSKOLANSKI, A.T. (1960). "Hydrometry : Theory and Practice of Hydraulic Measurements." Pergamon Press, Oxford, UK, 684 pages.

VALLENTINE, H.R. (1969). "Applied Hydrodynamics." *Butterworths*, London, UK, SI edition.